Transition Metal Chemistry
https://doi.org/10.1007/s11243-021-00471-7

Palladium(II) complexes of (*t*-butyl salicylidene) diphenyl disulfide diamine: synthesis, structure, spectral characterization and catalytic properties

Minu G. Bhowon[1] · **Sabina Jhaumeer Laulloo**[1] · **Eric C. Hosten**[2] · **Sumayya Elaheebacus**[1] · **Mounisha R. Dowlut**[1]

Received: 10 May 2021 / Accepted: 13 July 2021

Abstract

The hexadentate $N_2S_2O_2$ donor ligand N,N'-bis(3,5-*tert*-butylsalicylidene) diphenyl disulfide-2,2'-diamine was synthesised by the condensation of 2-aminophenyl disulfide and 3,5-di-*tert*-butyl-2-hydroxybenzaldehyde and its molecular structure was confirmed by X-ray studies. One of the *tert*-butyl groups in the Schiff base has rotational disorder around the C–C bond with ratio 0.56:0.44. The palladium complexes were prepared by the direct reaction of $PdCl_2(CH_3CN)_2$ and Schiff base ligands N,N'-bis (5-*tert*-butylsalicylidene) diphenyl disulfide-2,2'-diamine and N,N'-bis(3,5-*tert*-butylsalicylidene) diphenyl disulfide-2,2'-diamine, respectively. The structure of the metal complexes was characterized by physico-chemical and spectroscopic methods. Palladium is in square-planar geometry bonded to imine nitrogen and phenolic O in both the complexes. The catalytic efficiency of the palladium complexes was evaluated in the cross-coupling reactions; Heck-Mizoroki reaction of iodobenzene and methyl acrylate and the Suzuki-Miyaura reaction of phenylboronic acid and iodobenzene, which gave low to moderate yields. Higher conversions were obtained for **2a** as catalyst due to the increase in the number of bulky tertiary butyl groups in the structure.

Introduction

Palladium complexes have been used as catalysts in many cross-coupling organic reactions mainly for C–C bond formation such as Mizoroki-Heck and Suzuki-Miyaura due to their versatile nature [1–5]. These reactions have been extensively applied for the synthesis of natural products, bioactive compounds, pharmaceutical intermediates and industrial applications [6]. The palladium complexes bearing different ligand combinations such as phosphines [7, 8], imines [9], carbenes [10, 11], and thiols [12] have been reported to show moderate to good catalytic activity with various substrates. Phosphine-based ligands have been the preferred choice for C–C bond formation as they show many advantages [13]. However, the major drawbacks include the cost of the phosphine ligand itself, air and moisture-labilitye as well as being readily oxidized [14]. Schiff bases and their metal complexes continue to be of current interest for the design of catalysts. Schiff bases possess many advantages such as facile approach, relative tolerance, readily adjusted ancillary ligands, and tuneable steric and electronic coordination environments on the metal centre. Moreover, they can be synthesized both simply and cheaply in bulk amount, and their high thermal and moisture stabilities make them valuable catalysts in reactions carried out at high temperature. The interest with Schiff base ligands with N, O and S donating sites containing disulphide moiety has increased due to their capabilities of forming stable complexes of four, five or six co-ordinated metal complexes [15, 16]. In literature, there are not many disulfide-containing palladium Schiff base complexes displaying catalytic properties. Our interest in the synthesis of these types of disulphide metal complexes is due to contributions for materials chemistry in terms of molecular architectures, and development of new catalyst. Recently, we have reported the palladium disulfide complexes containing NS donor sites in the Mizoroki-Heck reactions, which have shown promising results [17]. The

---

✉ Minu G. Bhowon
mbhowon@uom.ac.mu

✉ Sabina Jhaumeer Laulloo
sabina@uom.ac.mu

[1] Department of Chemistry, Faculty of Science, University of Mauritius, Reduit, Mauritius

[2] Department of Chemistry, Nelson Mandela Metropolitan University, Summerstrand Campus South, Port Elizabeth, South Africa

presence of NOS donor sites in the studied ligand can influence the properties of complexes in terms of electronic and steric factors. Therefore, such systems are worth exploring as new catalyst for cross-coupling reactions.

Herein, we describe the synthesis and X-ray structure of Schiff base *N*,*N*′-bis(3,5-*tert*-butylsalicylidene) diphenyl disulfide-2,2’-diamine, **2**. The catalytic study efficiency towards the Heck-Mizoroki and the Suzuki-Miyaura reactions using the synthesised palladium complexes under different parameters were investigated.

Experimental

Materials and physical measurements

All the reagents and solvents were of analytical grade and were used without any purification. Bis(2-aminophenyl) disulphide, 3,5–di-*tert*-butyl-2-hydroxybenzaldehyde and the 5–*tert*-butyl-2-hydroxybenzaldehyde were purchased from Sigma-Aldrich Chemicals private Ltd. The FTIR spectra were recorded at the range of 400–4000 cm^{-1} using an Alpha-Bruker FTIR Diamond. CHNS elemental analyses were carried out using a Euro Vector EA-3000 CHNS analyzer. ^1H and ^{13}C NMR, DEPT, COSY AND HMBC spectra were obtained in $CDCl_3$ by using a Bruker electro spin 250 MHz Spectrometer. The UV-vis spectra were recorded in the range 200–800 nm using a Biochrom Libra S22 Spectrophotometer. The Fluorescence spectra were obtained on a Perkin Elmer LS55 fluorimeter. Mass spectra were recorded on a thermo Finnigan ESI-Ion trap using acetonitrile as solvent. A Perkin Elmer Clarus 560S GC-MS equipped with 30 m × 0.25 mm × 0.25 µm BPX35 capillary column, using the following oven temperature programme: 100 °C for 2.00 min, 150 °C/min up to 280 °C, and hold for 15.00 min.

Synthesis

The synthesis, characterisation and X-ray crystal structures of N,N’-bis(5-*tert*-butylsalicylidene)diphenyl disulphide-2,2’-diamine **1** has been reported earlier [18]. The NMR data for the different compounds are given in Table 1.

N,*N*′- Bis(3,5-tert-butylsalicylidene) diphenyl disulfide-2–2′-diamine, 2

Bis(2-aminophenyl) disulfide (1 mmol) and 3,5-bis(*tert*-butyl)-2-hydroxybenzaldehyde (2 mmol) were stirred in absolute ethanol (15 ml) and the resulting yellow precipitate formed after 4 days was filtered and dried under *vacuo*. Recrystallization with acetonitrile gave X-ray-grade crystals.

2: Colour: Yellow; Yield: (61%), Mp. 209.3–211.2 °C, Elemental analysis, Calc. (%) for $C_{42}H_{52}N_2O_2S_2$: C, 74.10; H, 7.64; N, 4.11; S, 9.41. Found: C, 73.54; H, 8.02; N, 4.33; S, 9.28. IR (ν/cm^{-1}): 2999, 2952 (O–H), 3067 (aromatic C-H), 2867, 2903 (CH_3), 1612 (C=N), 1054 (C-O), 748 (C–S), 510 (S–S). UV–Vis (λ (nm), log ε (dm^3 mol^{-1} cm^{-1})): (In DCM): 228.4 (80 211), 285.7 (53 920), 364.8 (36 560), (In Toluene): 285.4 (26 008), 363.3 (19 070).

Synthesis of metal complexes 1a, 2a

$PdCl_2(CH_3CN)_2$ was mixed with **1/2** in a 1:1 molar ratio in acetonitrile (35 ml) and NEt_3 (0.1 ml). The resulting solution was refluxed with stirring for 6 h followed with stirring for 1 week at room temperature. The resulting precipitate was filtered, washed successively with cold and hot acetonitrile and dried *in vacuo*.

1a: Colour: Orange; Yield: (56%), Mp. 331.4 °C, Elemental analysis, Calc. for $C_{34}H_{34}N_2S_2O_2$ Pd (727.24 g mol^{-1}): C, 56.15; H, 5.54; N, 3.85; S, 8.84. Found: C, 51.57; H, 4.22; N, 3.53; S, 8.60. IR (ν /cm^{-1}): 1589 (C=N), 2901–2864 ($C(CH_3)_3$), 742 (C–S), 1166 (C–O), 473 (S–S), 684 (Pd–O), 443 (Pd–N). UV-Vis (λ (nm), ε (M^{-1} cm^{-1}) (In DCM): 228 (33 484), 255 (36 171), 303 (18 009), 430 (8279).

2a: Colour Red; Yield 66%; Mp. 240 °C; Elemental analysis, Calc. for $C_{42}H_{50}N_2O_2S_2Pd$ (785.38): C, 64.23; H, 6.37; N, 3.57; S, 8.16. Found: C, 63.89; H, 6.96; N, 3.62; S, 7.94. IR (ν/ cm^{-1}): 1590 (C=N), 1055 (C–O), 747 (C–S), 516 (S–S), 656 (Pd–O), 447 (Pd–N). UV-Vis (λ (nm), ε (M^{-1} cm^{-1}) (DCM): 227 (54,066), 255 (40,666), 437 (9000). FAB-mass m/z, 785.25 $[Pd[C_{42}H_{50}N_2O_2S_2]]^{+\cdot}$, 726.60 $[Pd[C_{38}H_{41}N_2O_2S_2]]^{+\cdot}$, 681.35$[C_{42}H_{50}N_2O_2S_2]^{+\cdot}$.

X-ray diffraction study

X-ray diffraction studies were performed at 200 K using a Bruker Kappa Apex II diffractometer with graphite monochromated Mo Kα radiation ($\lambda = 0.71069$ A). APEXII was used for the data collection and SAINT for cell refinement and data reduction [19]. Data were corrected for absorption effects using the multi-scan method in TWINABS [19]. The structures were solved by dual methods with SHELXT-2018/2 [20] and refined by least squares procedures using SHELXL-2018/3 [21], with SHELXLE [22] as a graphical interface. Three reflections with large differences between their observed and calculated intensities were omitted. All non-hydrogen atoms were anisotropically refined. Carbon-bound hydrogens were placed in calculated positions and were included in the refinement in the riding model approximation, with U_{iso}(H) set to $1.2U_{eq}$(C). The hydrogen atoms of the non-disordered methyl groups were allowed to rotate with a fixed angle around the C–C bond to best fit the experimental electron density (HFIX 137 in the SHELXL programme [21]) with U_{iso}(H) set to $1.5U_{eq}$(C). The hydrogen atoms of the disordered methyl groups were

Table 1 Spectral data of **1**, **2**, **1a** & **2a**

Atom	1		1a				2		2a			
	δ_H (J Hz)	δ_C ppm	δ_H (J Hz)	δ_C ppm	COSY	HMBC	δ_H (J Hz)	δ_C ppm	δ_H (J Hz)	δ_C ppm	COSY	HMBC
1	8.63 s	163.5	7.69 s	152.4		9, 2, 8, 13	8.64	164.1	8.48 s	155.1		9, 2, 8, 13
2	–	146.6	–	150.1	–	–	–	146.6	–	149.7	–	
3	–	131.6	–	135.6	–	–	–	131.6	–	136.8	–	–
4	7.65 (dd, 7.5, 1.7)	127.2	7.90–7.86 (d, 7.8)	133.2	5	2, 6	7.66–7.63 (dd, 7.3, 1.8)	127.1	7.98–7.95 (d, 7.8)	133.6	5	2, 6
5	7.16 (td, 7.0, 1.7)	127.2	7.10–7.04 (td, 7.8, 2.0)	127.4	4, 6	3, 7	7.18–7.11 (td, 7.3, 1.8)	127.4	7.15–7.09 (t, 7.8)	126.9	4, 6	3
6	7.16 (td, 7.0, 1.7)	127.5	7.22–7.21 (m)	126.8	5, 7	2, 4	7.18–7.11 m	126.8	6.96–6.92 (td, 8.0, 2.5)	126.4	5, 7	2, 4
7	7.23 (dd, 7.0, 1.7)	117.7	7.22–7.21 (m)	116.1	6	3, 5	7.21–7.18 (dd, 7.3, 1.8)	117.7	7.56–7.52 (d, 8.4)	115.7	6	3, 5
8	–	118.4	-	118.7			–	118.7	–	119.0		
9	12.64	158.9	–	162.5			13.17 s	158.4	–	163.4		
10	7.02 (d, 8.0)	117.1	6.57–6.53 (d, 9.0)	122.8	11	12, 8	–	137.3	–	136.0		
11	7.47 (dd, 8, 2.4)	131.2	7.46–7.41 (dd, 9.0, 2.6)	134.2	10	9, 13	7.22–7.24 (d, 2.0)	127.4	6.96–6.92 (s)	129.1		
12	–	141.9	–	137.1				140.7	–	140.3		
13	7.40 (d, 2.40	128.9	6.72–6.71	129.8		1, 9, 11	7.47–7.46 (d, 2.2)	128.6	7.33–7.32 (d, 2.2)	130.9		
14	–	34.1	–	33.8	–		–	35.2	–	33.8		
15,16,17	1.34	31.4	1.28	31.8			1.47 s	29.4	1.29 s	31.3		
18	–	–	–	–			–	34.2	–	35.6		
19, 20, 21	–	–	–	–			1.43 s	31.5	1.25 s	30.0		

placed in calculated positions. The hydrogen atoms of the hydroxyl groups were allowed to rotate with a fixed angle around the C–O bond to best fit the experimental electron density (HFIX 147 in the SHELXL programme [21]), with U_{iso}(H) set to 1.5U_{eq}(O).

General procedure for Mizoroki-Heck reaction

Aryl halide (1 mmol), octadecane (1 ml, 50 mg/ml), methyl acrylate (2 mmol), base (2.4 mmol), **1a/2a** (1 mmol %) and DMF (5 ml) were heated to 120 ℃ in an oil bath in a closed boiling tube for 18 h. 1 ml of the reaction mixture was diluted to 5 ml with DCM and was analyzed by GC.

General procedure for Suzuki–Miyaura reaction

Iodobenzene (1.0 mmol), phenyl boronic acid (1.5 mmol), K_2CO_3 (2.0 mmol), **1a/2a** (1 and 2 mmol%), octadecane as internal standard (0.3 mmol) in DMF (5 mL) were heated in a sealed tube in an oil bath of 120 °C for 18 h. The reaction mixture was diluted with DCM to 2 ml and analyzed using GC-MS.

Results and discussion

Synthesis

The suitable single crystals of *N*,*N*'-bis(3,5-*tert*-butyl-salicylidene) diphenyl disulfide-2-2'-diamine, **2** was obtained by slow evaporation of acetonitrile solution over a period of one week and its structure was determined by X-ray crystallography. The palladium complexes **1a–2a** were obtained on reacting the Schiff bases **1–2** with $PdCl_2(CH_3CN)_2$, in acetonitrile (Scheme 1). Both complexes were found to be air stable and were soluble in DCM, chloroform and DMSO. Suitable single crystals could not be grown for the complexes. However, the obtained elemental analyses and 2D NMR spectra were in good agreement with the suggested structures where, one mole of the Schiff bases containing N_2O_2 donor atoms are co-ordinated to the palladium centre with no S–S bond cleavage.

Crystal structure of 2

The molecular structure of **2** with atom labelling is given in Fig. 1. Crystallographic data, data collection parameters and details of the refinements are given in Table S1. The crystal studied was refined as a two-component twin (BASF = 0.282(2)). One of the *tert*-butyl groups has rotational disorder around the C–C bond with ratio 0.56:0.44. The disulfide single bond length was found to be 2.025(2) Å (S1–S2) with bond S2–S1–C22 and S1–S2–C32 angles of 104.0(2)° and 104.8(2)°, respectively. The C=N bond distance of **2** is 1.265(7)–1.271(7) Å which is in accordance to the reported C=N bond length in salicylaldiminato [23]. The torsion angles of C22–S1–S2–C32, S2–S1–C22–C21, S2–S1–C22–C23, S1–S2–C32–C31 and S1–S2–C32–C33 were found to be 80.8(3)°, 173.4(4)°, – 4.4(5)°, – 175.7(4)° and 2.6(5)°, respectively. One of the salicylideneaniline groups is planar with a least square plane rms deviation of 0.0177 through the non-hydrogen atoms. In contrast, the phenyl ring of the other salicylideneaniline is rotated by 54.9(2) ° at N2. Strong intra-molecular bonding of

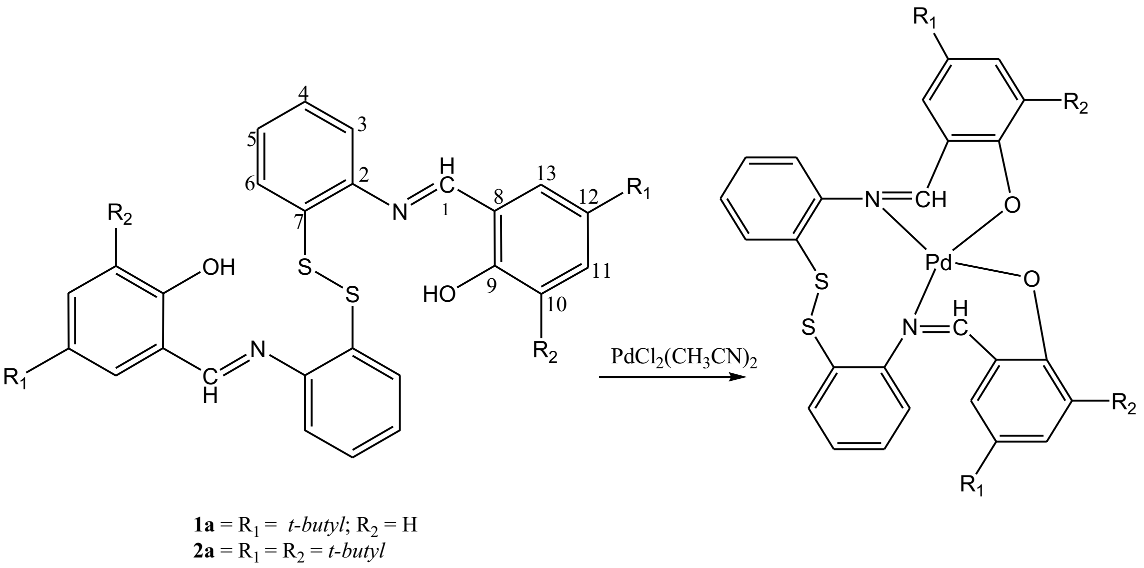

Scheme 1 Formation of the palladium complexes **1a** & **2a**

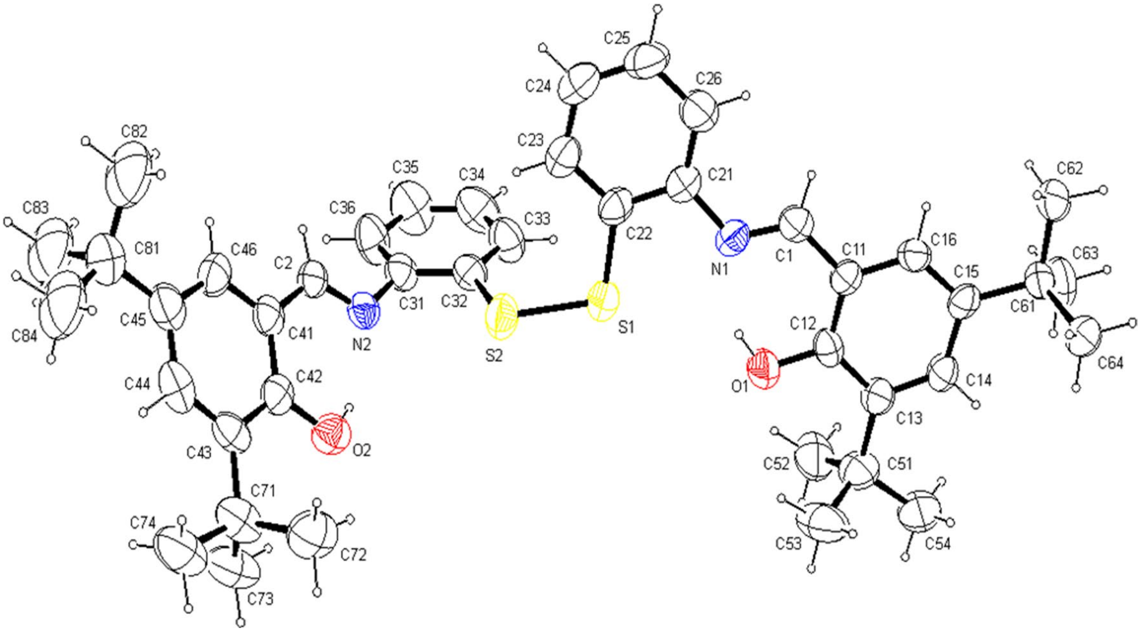

Fig. 1 Asymmetric unit of **2**. Ellipsoids drawn at 50% probability and minor disordered components are not shown

O1–H1A…N1 and O2–H2A…N2 was observed with HN distance of 1.88 Å and angles of 148° and 145°, respectively. Inter-molecular interactions include two π…π ring interactions between the rings C11–C16 and C21-C26 of length 3.903(4) Å and slippage of 1.814 and 1.727 Å. Two long inter-molecular C–H…π ring interactions of 2.88 and 2.96 Å occur. Selected bond lengths, bond angles, torsion angles and hydrogen-bonding data are presented in Tables S2 and S3 respectively.

Spectral data

In the IR spectra of the free ligands (**1**, **2**), the phenolic OH appeared as medium peak at 2978–2999 and 2952–2959 cm^{-1} which suggested strong inter-molecular hydrogen bonding between OH and the nitrogen of the azomethine group [18]. The symmetric and asymmetric stretching vibration bands of *tert*-butyl appeared in the region of 2867–2904 cm^{-1}. The characteristic stretching frequencies at 1607, 738 and 1612 cm^{-1}, 748 cm^{-1} for the azomethine υ(C=N) and υ(C–S) in **1** and **2**, shifted to 1589, 1590 cm^{-1} [24] and 742, 747 cm^{-1} in the complexes **1a** and **2a** due to coordination of nitrogen to the metal centre. The peaks at 684, 635 and 443, 424 cm^{-1} were due to Pd–O and Pd–N respectively [25].

The disappearance of the peaks at δ 12.80, 13.17 ppm in the ^{1}H NMR spectra of **1a** and **2a** indicated deprotonation and coordination of oxygen atom to palladium. The azomethine protons at 8.61, 8.64 ppm shifted upfield in the complexes. The tertiary butyl groups in the metal complexes shifted upfield due to the anisotropic effect triggered by close proximity to the aromatic rings [26].

In the ^{13}C NMR spectra of complexes, the azomethine carbons shifted upfield compared to the free ligands, while the tertiary phenolic carbon shifted downfield.

The complete assignment of different protons and carbons in **1a** and **2a** is based on 2D NMR data (Table 1). The chemical shift values of different carbons are based on the HSQC spectra. The chemical shift value of carbons 2 and 6 is established via the HMBC correlations from H_4 while that of C_3 and C_7 via the correlation with H_5. In addition, the imine proton is found to correlate with chemical shift values of C_9, C_{13}, C_2 via ^{3}C–H and weak interactions with C8 via ^{2}C–H. The COSY, HSQC and HMBC spectra of **1a** are illustrated in Fig. 2. (i, ii, iii).

The molecular ion peak of **2a** at m/z 787.2582 (785.3593) corresponded to the molecular formula $Pd[C_{42}H_{50}N_2O_2S_2]$. The fragment ion at m/z 681.3579 (680.9376) corresponded to the free ligand (**2**) indicating no cleavage of the S–S bond.

The Schiff bases **1** and **2** exhibited three intense absorption bands at 230 and 228, 269 and 286 nm, 352 and 364 nm due to intraligand $\pi \rightarrow \pi^*$ and $n \rightarrow \pi^*$ charge transfer of the aromatic rings and imine groups, respectively, in the electronic spectroscopy. Unlike, many other aryl salicylaldimine derivatives there was no absorption above 400 nm suggesting that **1** and **2** both exist only in enol-imine tautomer form at room temperature [18, 27]. The three absorption bands shifted to 227, 255 and 303 nm in the palladium complexes.

Fig. 2 (i) COSY spectra of **1a**; (ii) HSQC spectra of **1a;** (iii) HMBC spectra of **1a**

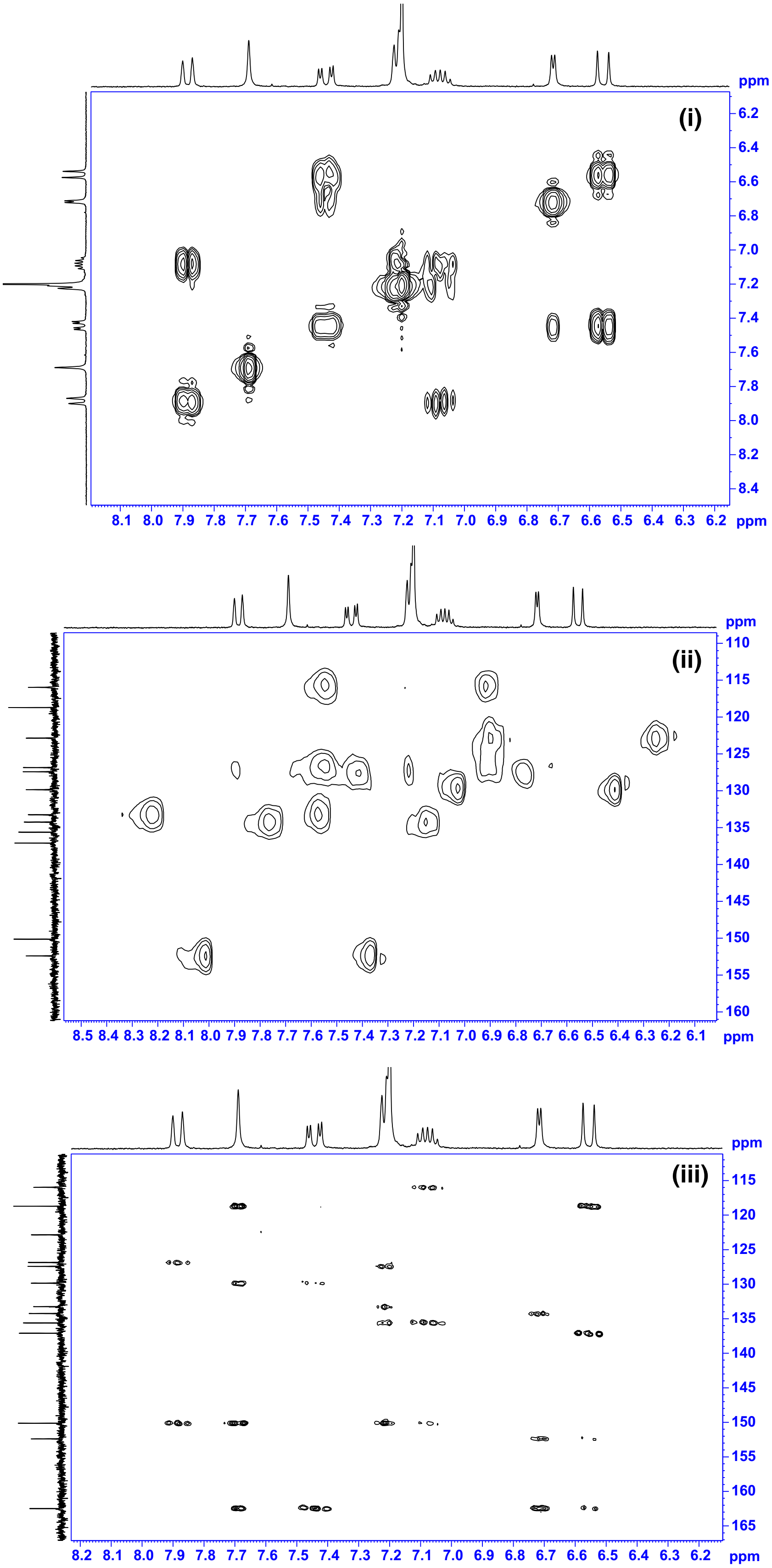

The metal to ligand charge transfer occurred at ~ 430 nm, which was indicative of a square-planar geometry [27].

Catalytic activity

Palladium-catalyzed C–C bond-forming reactions are important for the synthesis of biphenyls, which are important intermediates for many organic molecules. Hence, **1a** and **2a** were explored as catalyst in the Mizoroki-Heck and Suzuki-Miyaura reactions. **2a** was employed to explore the various parameters such as catalyst loading, time, temperature, base system and solvent.

The phenyl acrylates were obtained in moderate yields in Mizoroki-Heck reactions using methyl acrylate and aryl iodide/4-bromobenzaldehyde. When the reaction was carried out using 0.1–2 mmol %, the yield of the product increases from 55 to 75% (entry 2–4). No significant difference was observed on increasing the catalyst loading from 1 to 2 mmol %; hence, further reactions were carried out using 1 mmol % catalyst loading. The optimum reaction time for the reaction was 18 h and Na_2CO_3 as base. When the reaction was carried out at 50 and 70 °C, no product was formed. On varying the temperature, the yield increases up to 70% but no significant increase was observed on further increasing the temperature from 120 to 170 °C (Table 2). On using polar solvents such as water, ethanol, no conversion was observed.

Higher conversions for the product were obtained for **2a** compared to **1a** as catalyst due to the increase in the number of bulky tertiary butyl groups in the structure which are presumed to enhance the oxidative and reductive steps [28].

1a and **2a** were not found to be efficient catalyst for the coupling of aryl iodide/4-bromobenzaldehyde and phenylboronic acid (Suzuki reaction) and the maximum yield obtained was only 44% (Table 3).

Conclusion

In this work, hexadentate Schiff bases and their palladium complexes were synthesised and characterized fully using 2D NMR spectra. Palladium(II) complexes have square-planar geometry co-ordinated to nitrogen and oxygen without S–S bond cleavage-bearing bulky substituents on the aromatic ring and act as catalyst for Mizoroki-Heck and Suzuki-Miyaura reactions. Good conversions were obtained in Mizoroki-Heck reaction when carried out at 120 °C in Na_2CO_3 as base. However, both the complexes were not that effective for the conversion in Suzuki-Miyaura reaction. **2a**

Table 2 Catalytic activity of palladium complexes in Mizoroki-Heck reaction

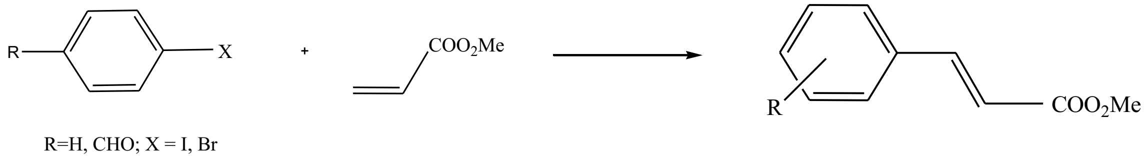

Entry	Aryl halide	Catalyst	Catalyst loading (mmol %)	Time (h)	Temp(°C)	Base	Solvent	Yield[a] (%)	TON[a,b]
1	Iodobenzene	2a	0.1	18	120	Na_2CO_3	DMF	55	443
2	Iodobenzene	2a	1	18	120	Na_2CO_3	DMF	70	62
3	Iodobenzene	2a	2	18	120	Na_2CO_3	DMF	75	33
4	Iodobenzene	2a	1	24	120	Na_2CO_3	DMF	68	62
5	4-Bromobenzaldehyde	2a	1	18	120	Na_2CO_3	DMF	77	86
6	4-Bromobenzaldehyde	2a	1	24	120	Na_2CO_3	DMF	48	65
7	Iodobenzene	2a	1	18	100	Na_2CO_3	DMF	36	28
8	Iodobenzene	2a	1	18	120	Na_2CO_3	DMF	71	65
9	Iodobenzene	2a	1	18	140	Na_2CO_3	DMF	69	55
10	Iodobenzene	2a	1	18	170	Na_2CO_3	DMF	54	47
11	Iodobenzene	2a	1	18	120	NaOH	DMF	45	45
12	Iodobenzene	2a	1	18	120	K_2CO_3	DMF	67	60
13	Iodobenzene	1a	1	18	120	Na_2CO_3	DMF	58	30

Reaction conditions: Aryl halide (1.0 mmol), methyl acrylate (2.0 mmol), base (2.4 mmol), solvent (5 mL)

[a] The reported values are the average of those of two samples

[b] TON is given as moles of product per mole catalyst

Table 3 Catalytic activity of complexes in Suzuki-Miyaura reaction

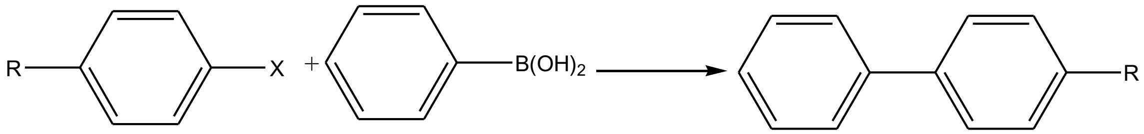

X= I ,Br
R=H, CHO

Entry	Aryl halide	Catalyst	Catalyst loading (mmol %)	Time (h)	Temp (°C)	Base	Solvent	Yield[a] (%)	TON[a,b]
1	Iodobenzene	2a	0.1	18	120	K_2CO_3	DMF	34	3
2	Iodobenzene	2a	1	18	120	K_2CO_3	DMF	44	43
3	Iodobenzene	2a	1	5.5	120	Na_2CO_3	DMF	18	18
4	Iodobenzene	2a	1	24	120	Na_2CO_3	DMF	41	41
5	4-Bromobenzaldehyde	2a	1	18	120	K_2CO_3	DMF	1	1
6	Iodobenzene	2a	1	18	100	K_2CO_3	DMF	39	40
7	Iodobenzene	2a	1	18	120	NaOH	DMF	3	3
8	Iodobenzene	2a	1	18	120	Na_2CO_3	DMF	40	41
9	Iodobenzene	1a	1	18	120	K_2CO_3	DMF	28	28
10	Iodobenzene	1a	2	18	120	K_2CO_3	DMF	30	15

Reaction conditions: Aryl halide (1.0 mmol), phenylboronic acid (1.5 mmol), base (2 mmol), solvent (5 mL)

[a] The reported values are the average of those of two samples

[b] TON is given as moles of product per mole catalyst

was a more efficient catalyst compared to **1a** for both reactions due to the presence of two *tert*-butyl groups.

CCDC 2,018,397 contains the supplementary crystallographic data for this paper. These data can be obtained free of charge from The Cambridge Crystallographic Data Centre via www.ccdc.cam.ac.uk/structures.

Supplementary Information The online version contains supplementary material available at https://doi.org/10.1007/s11243-021-00471-7.

Funding The authors receive support from University of Mauritius Grant for the submitted work.

Declarations

Conflict of Interest The authors have no conflict of interest to declare that are relevant to the content of this article.

References

1. Wu XF, Anbarasan P, Neumann H, Beller M (2010) Angew Chem Int Ed Engl 49(48):9047–9050
2. Fernández E, Rivero-Crespo MA, Domínguez I, Rubio-Marqués P, Oliver-Meseguer J, Liu L, Cabrero-Antonino M, Gavara R, Hernández-Garrido JC, Boronat M, Leyva-Pérez A, Corma A (2019) J Am Chem Soc 141(5):1928–1940
3. Agrahari B, Layek S, Ganguly AR, Pathak DD (2018) Inorg Chim Acta 471:345-354
4. Kim MJ, Jung MJ, Kim YJ, Sung HK, Lee JY, Sung JH, Park CP (2018) Tetrahedron Lett 59(31):2989–2993
5. Veerasamy N, Munusamy S, Muniyappan P, Dhananjayan K, Venkatachalam G, Balasubramani K (2020). J Organomet Chem. https://doi.org/10.1016/j.jorganchem.2020.121220
6. Seechurn CCJ, Kitching MO, Colacot TJ, Snieckus V (2012) Angew Chem Int Ed 51:5062–5085
7. Cheisson T, Auffrant A (2016) Dalton Trans 45:2069–2078
8. Ratnam A, Bala M, Kumar R, Singh UP, Ghosh K (2018) J Organomet Chem 856:41–49
9. Keleş M, Keleş H, Emir DM (2015) Appl Organomet Chem 29(8):543–548
10. Kim S, Cho HJ, Shin SD, Lee MS (2017) Tetrahedron Lett 58:2421–2425
11. Begum T, Mondal M, Borpuzari MP, Kar R, Kalita G, Gogoi PK, Bora U (2017) Dalton Trans 46:539–546
12. Feng XJ, Yan M, Zhang T, Liu Y, Bao M (2010) Green Chem 12:1758–1766
13. Park CH, Kwon YJ, Oh IY, Kim WS (2017) Adv Synth Catal 359:107–119
14. Shahnaz N, Banik B, Das P (2013) Tetrahedron Lett 54(22):2886–2889
15. Bharti S, Choudhary M, Mohan B, Rawat SP, Sharma SR, Ahmad K (2018) J Mol Struct 1164:137–154
16. Moosun S, Jhaumeer Laulloo S, Bhowon MG (2013) J Mol Struct 1053:106–114

17. Moosun SB, Blair LH, Coles SJ, Bhowon MG, Jhaumeer-Laulloo S (2017) J Saudi Chem Soc 21(4):441–449
18. Bhowon M, Jhaumeer Laulloo S, Hosten E, Khodabaccus M, Ryhman L, Ramasami P (2018) J Mol Struct 1175:13–23
19. Bruker (2007) APEX2, SAINT, TWINABS. Bruker AXS Inc., Madison, Wisconsin, USA
20. Sheldrick GM (2015) Acta Cryst A71:3–8
21. Sheldrick GM (2015) Acta Cryst C71:3–8
22. Hübschle CB, Sheldrick GM, Dittrich BJ (2011) Appl Cryst 44:1281–1284
23. Ahmad JU, Räisänen MT, Nieger M, Sundberg MR, Figiel PJ, Leskelä M, Repo T (2012) Polyhedron 38(1):205–212
24. Shafaatian B, Baharian A (2017) Phosphorus Sulfur Silicon Relat Elem 192(10):1102–1109
25. Kumar S, Solanki A, Kundu S (2017) J Mol Struct 1143:163–167
26. Kasumov V, Sahin E (2013) Spectrochim Acta A Mol Biomol Spectrosc 107:31–38
27. Kasumov V, Uçar I, Bulut A (2010) J Fluor Chem 131(1):59–65
28. Tianzhu Z, Dawei G, Suyun J, Wen-Hua S, Li T, Xiaozhen Y (2004) J Polym Sci A Polym Chem 42(19):4765–4774